



The use of carbon lubricants with different morphologies in boron oil on tribological performance of AlSi16 alloy

AlSi16 alaşımının tribolojik performansına farklı morfolojilerdeki karbon yağlayıcılarının bor yağı içinde kullanımı

Zafer Sahin¹ , Hamza Simsir^{2,*} 

¹ Department of Metallurgical and Materials Engineering, Karabuk University, 78050, Karabük, Türkiye.

² Metallurgy Program, TOBB Technical Science Vocational School, Karabuk University, Karabük 78050, Türkiye.

Abstract

This study examined the impact of carbon-based lubricants, utilized as solid lubricants to reduce material wear rates. Graphite, carbon nanotubes, and two hydrothermal carbons were incorporated into boron oil to prepare colloidal suspensions for this objective. To evaluate the concentration effect, three different ratios of each carbon lubricant were used. AlSi16 alloy, which is frequently exposed to wear in a range of application areas, was used as the substrate material in wear studies. There was a detailed discussion of the wear processes and the results. These discussions showed that smaller particle shapes produced better results and that the wear rate of the substrate material decreased as the carbon lubricant content increased. It was found that the wear rate of the AlSi16 substrate material was reduced by more than 70% when carbon nanotubes and two hydrothermal carbons (0.2 weight percent) were used.

Keywords: Tribology, Carbonaceous lubricant, Al-Si alloy, Wear mechanism.

1 Introduction

A critical factor in determining the durability and efficiency of mechanical systems is wear, defined as the gradual loss of material or gradual material from a surface due to mechanical interaction with the environment. It significantly affects the lifetime and performance of the system and occurs under various conditions. Fatigue wear is classified as erosive, erosive-abrasive, adhesive, and generally adhesive. Adhesive wear occurs when material transfer results from the bonding of surface roughness, while abrasive wear is caused by the shearing or sliding action of harder particles on a softer surface. Erosion wear occurs when particles or liquids strike a surface, and fatigue wear results from cyclic loading and unloading that causes surface cracking. A thorough knowledge of these mechanisms is important for the design of wear-resistant materials and components [1-4].

Aluminum-silicon (Al-Si) alloys are widely used in industries such as automotive and aerospace due to their superior mechanical properties, excellent corrosion resistance and low density. They are used in the manufacture

Öz

Bu çalışmada, malzemenin aşınma hızını azaltmak için katı yağlayıcı olarak kullanılan karbon bazlı yağlayıcıların etkisi incelenmiştir. Bu amaçla, grafit, karbon nanotüpler ve iki hidrotermal karbon, bor yağına katılarak koloidal süspansiyonlar hazırlanmıştır. Konsantrasyon etkisini değerlendirmek için, her bir karbon yağlayıcının üç farklı oranı kullanılmıştır. Aşınma çalışmalarında, çeşitli uygulama alanlarında sık sık aşınmaya maruz kalan AlSi16 alaşımı, alt tabaka malzemesi olarak kullanılmıştır. Aşınma süreçleri ve sonuçları ayrıntılı olarak tartışılmıştır. Bu tartışmalar, özellikle daha küçük parçacık şekillerinin daha iyi sonuçlar ortaya koyduğunu, karbonlu yağlayıcı içeriği arttıkça alt tabaka malzemesinin aşınma hızının azaldığı gösterdi. Karbon nanotüpler ve iki hidrotermal karbon (ağırlıkça yüzde 0.2) kullanıldığında AlSi16 alt tabaka malzemesinin aşınma oranının %70'ten fazla azaldığı bulunmuştur.

Anahtar kelimeler: Triboloji, Karbonlu yağlayıcı, Al-Si alaşımı, Aşınma mekanizması

of various engine components such as cylinder blocks, pistons, piston joint rings, cylinder liners, and cylinder heads, where adhesive wear (or dry sliding wear) predominates [5, 6]. The presence of silicon particles in the aluminum matrix significantly improves the wear resistance of these alloys by reducing surface deformation during sliding and providing a rigid reinforcement. The wear behavior of Al-Si alloys is generally abrasive and adhesive mechanisms. Abrasive wear occurs when silicon particles prevent the penetration of harder particles and thus reduce material loss. On the other hand, adhesive wear leads to local material transfer when Al-Si alloys interact with softer counter surfaces [1, 7, 8].

Lubricants play a critical role in reducing wear and friction between interacting surfaces by forming a protective layer that prevents direct contact. Temperature, load, sliding speed, and impurities are some of the factors that affect the tribological performance of lubricants. High temperatures can cause liquid lubricants to degrade but can also cause some solid lubricants to become self-lubricated. Similarly, sliding speed determines heat generation and lubricant

* Corresponding author, e-mail: hamzasimsir@karabuk.edu.tr (H. Simsir)
Received: 20.05.2025 Accepted: 12.01.2026 Published: 05.02.2026
doi: 10.28948/ngumuh.1702583

behavior, while the applied load affects the thickness and stability of the lubricating film [1, 3, 9]. Graphite, molybdenum disulfide (MoS₂), and polytetrafluoroethylene (PTFE) are examples of solid lubricants known for their effectiveness in harsh environments where liquid lubricants often fail. These materials remove surface imperfections and minimize wear by forming a protective layer that reduces friction and prevents direct metal-to-metal contact [10, 11].

Graphene, carbon nanotubes (CNTs), and fullerenes are examples of carbon-based solid lubricants that have attracted much interest due to their outstanding mechanical, thermal, and chemical properties [1, 12]. A number of variables, such as surface shape, environmental parameters, and the presence of functional groups, influence how well carbon-based solid lubricants work. For example, graphene oxide, a graphene derivative, has shown better tribological capabilities as it can form stable films under sliding conditions [13–15]. Furthermore, biomass-based hydrothermal carbon (HTC) is becoming a viable and affordable alternative to premium carbon sources. HTC is suitable for industrial applications due to its exceptional thermal stability and ability to maintain lubrication performance at high temperatures [16]. However, there are almost no known studies in the literature where it has been used as a solid lubricant [3].

This work examined the tribological characteristics of AlSi16 in boron oil after adding solid carbon lubricants with four different morphological shapes. Wear mechanisms were used to thoroughly explain the consequences of surface profilometer images, SEM and SEM-EDX investigations, and wear rate computations.

2 Experimental section

2.1 Preparation of Al-Si 16 alloy substrate and HTCs

The wear test in this work was conducted using the Al-Si 16 alloy, which has a hardness of 75.8 ± 4.6 Hv and a chemical composition listed in Table 1. For wear and microstructure investigations, the samples underwent cutting, sanding, and polishing procedures. To sand the samples, 400-, 600-, 800-, 1200-, and 2000-grit sandpaper with water reinforcement was used in that order. Traces from the previous sanding were eliminated by rotating the specimen at a 90° angle at the transition between each sanding. Polishing felt was used to polish after sanding. The polishing abrasive utilized was an alumina solution. Following the procedure, clean water was used to wash and then dry the sample surface.

Table 1. The chemical composition of AlSi16 Alloy

Elements	Si	Fe	Mg	Mn	Cu	Zn	Al
Content (wt%)	16.37	0.53	0.28	0.10	0.07	0.05	Balance

A 50 ml Teflon container containing 1.5 g of glucose (Sigma-Aldrich) and chitosan (Merck) was put in two different stainless steel autoclaves. After that, 20 milliliters of deionized water were added. After closing the autoclave, it was baked for 30 hours at 210 °C. After being taken out of

the oven, the autoclave was allowed to cool to room temperature. After that, 300 ml of deionized water was used to wash the solid and liquid combination before it was filtered through filter paper. After two hours of drying at 105 °C, the solid carbons that were still present on the filter paper were kept. The experimental conditions were determined by reviewing previous studies [16, 17].

2.2 Wear test and characterization

The UTS Tribometer T10/20 abrasion tester, which includes both rotating and reciprocating motion modules, was used to perform the abrasion test in a pin-on-disc configuration (Figure 1). The worn specimens measured 3 mm in height and 5 x 6 mm in length and width. The specimens traveled 3000 meters, with a sliding distance at room temperature, a load of 50 N, and at a wear rate of 3 mm/s. Four distinct carbons with solid lubricating qualities and a 5 wt% boron oil suspension were employed as wear lubricants. These carbons include HTCs with two different morphologies (derived from glucose and chitosan), expandable graphite (Nanography, purity: 95-97% and size: 50 mesh), and multi-walled carbon nanotubes (Nanography, purity: > 92%, outside diameter: 7-16 nm). The abbreviations for these carbons are Htc-C, Htc-G, Grpht and Cnt, respectively. Wear experiments were conducted after each carbon lubricant was introduced to boron oil in three different ratios (0.05, 0.1, and 0.2 wt% oil). Boron oil provides a suitable, stable, and controllable lubrication environment. Unlike industrial oils containing complex additives, boron oil has a simpler chemical composition, which allows the tribological impact of carbon-based additives to be evaluated without interference [18]. All suspensions were first stirred at room temperature for 4 hours at 700 rpm in a magnetic stirrer to allow the large carbon particles to disperse. Subsequently, to increase the homogeneous distribution within the suspension and minimize agglomeration, all suspensions were stirred for 2 hours in an ultrasonic bath at 50°C. No sedimentation occurred in the suspension due to the addition of carbonaceous lubricant at very low concentrations. At the end of each test, the suspensions and balls containing solid lubricant were replaced. Wear testing was conducted using 6 mm-diameter AISI 52100 stainless steel balls.

The applied load results in Hertzian contact pressures of 2-5 MPa in standard pin-on-disk configurations utilizing Al-Si pins, consistent with lubrication pressures in piston-cylinder interfaces characterized by dominant asperity contact and thin lubrication films. The sliding speed resembles low-speed movement in piston rings during the starting and idling stages. The sliding distance corresponds to hours of total operation, adequate for consistent wear in pistons without the need for complete engine cycles, as confirmed in hypereutectic Al-Si studies [19, 20].

Using a Mitutoyo SJ-410 profilometer, the area of the worn surfaces following the wear tests was determined. Using the Archard coefficient and Equation 1, the wear rate was determined. Where W_v is worn volume (mm³) and l is the sliding distance (m). The Carl Zeiss Ultra Plus Gemini FESEM model scanning electron microscope equipped with

an energy dispersive X-ray (EDX) spectrometer was used to analyze the scars that developed following the wear test to identify the wear process.

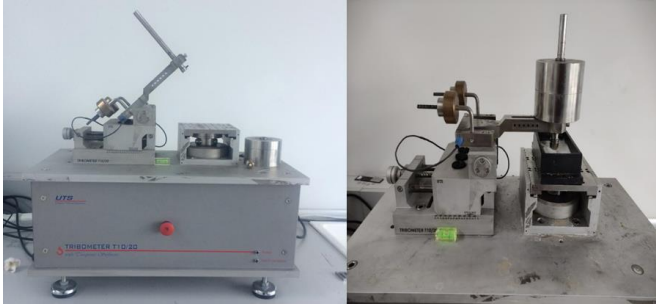


Figure 1. UTS Tribometer wear tester

A Thermo Scientific Nicolet iS50 FTIR-ATR Fourier transform infrared spectrometer was used to examine the functional groups of carbons. Six scans with a spectral resolution of 1 cm⁻¹ were used to generate FTIR spectra in the wavenumber range of 4000 to 600 cm⁻¹.

$$\text{Wear Rate} = W_v/l \quad (1)$$

3 Result and discussion

Figure 2 shows SEM pictures of the Grpht, Htc-C, Htc-G, and CNT carbon-based materials utilized in wear tests. It was found that Grpht had a geometrically irregular flake morphological structure. HTC-C had a fiber structure with bumps on it, HTC-G had a spherical morphology with a diameter of 846 ± 92 nm, and CNT was made up of nano-sized tubes and a fiber structure.

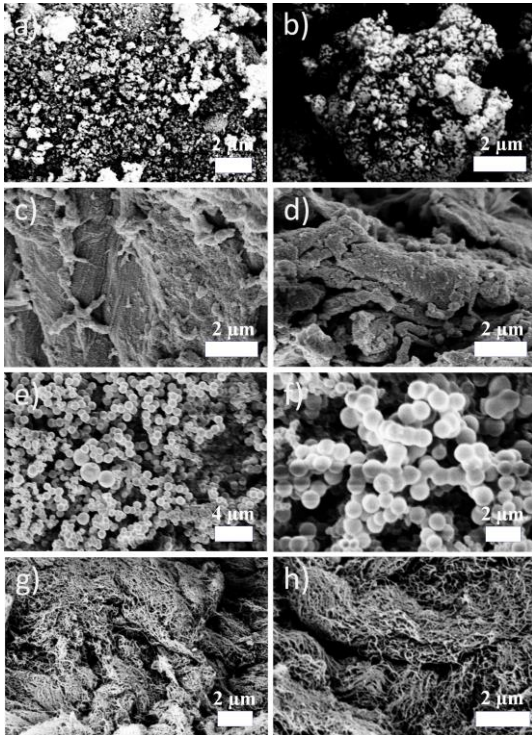


Figure 2. SEM images of carbon-based lubricant additives a-b) Grpht, c-d) Htc-C, e-f) Htc-G, and g-h) CNT

Figure 3 displays the FTIR spectra of the carbon materials utilized in wear tests, including Grpht, Htc-C, Htc-G, and CNT. All carbons showed peaks at wavelengths of (C-C) 1013 cm⁻¹, (C-O) 1050 cm⁻¹, (C=O) 1685 cm⁻¹, (C=N) 2315 cm⁻¹, (C-H) 2973 cm⁻¹, and (OH) 3737 cm⁻¹. In HTC-C, there is a decrease in the intensity of the (C=O) 1685 cm⁻¹ peak, while the intensity of the (C=N) 2315 cm⁻¹ peak is high due to the amine group present in the structure of chitosan. The (C=N) 2315 cm⁻¹ peak's strength significantly dropped at the Htc-G, whereas the (OH) 3281 cm⁻¹ peak widened and became more noticeable. For Grpht and CNT, the high intensity of the (C=O) 1685 cm⁻¹ peak is thought to be due to oxidized layers in the structure. The results gained align with the research that has been published in the literature [16, 21].

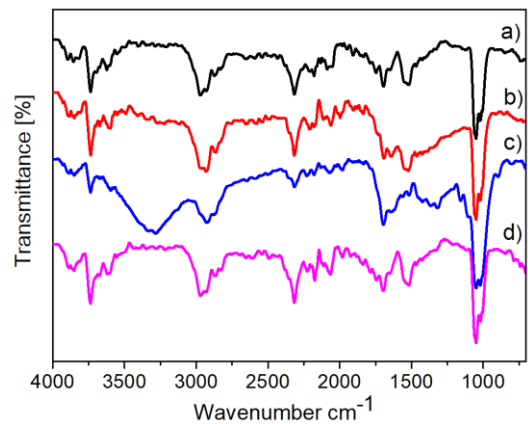


Figure 3. FT-IR spectra of the carbons a) Grpht, b) Htc-C, c) Htc-G, and d) CNT

Figure 4 illustrates how the type of solid lubricant affects the AlSi 16 substrate material's wear rates. Analysis of the data shows that when the solid lubricants were added to boron oil and the amount of carbon increased, the wear rates dramatically lowered. This can be attributed to the lubricants' formation of a protective tribofilm on the substrate material's surface [22, 23]. Some of the solid lubricant will break up and separate and settle in the gaps between the rough areas. Consequently, until the roughness is eliminated, this mechanism will continue to work.

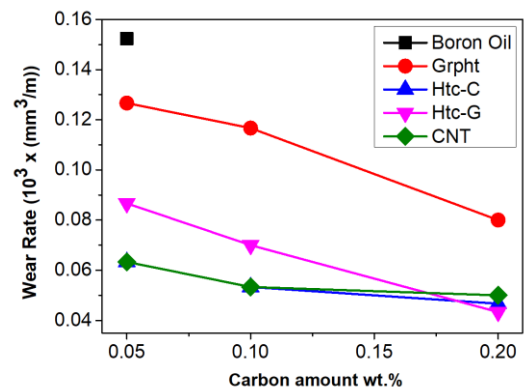


Figure 4. Wear rates of the substrate material according to the type and amount of carbon-based lubricant

The findings showed that, in comparison to other carbons, Htc-C and CNT made of nanosized agglomerated spheres and tubular formation performed better, particularly when added at low amounts. Although not visible in the SEM images, the nano-sized agglomerated sphere structure on the HTC-C surface, similar to the nano-sized tube structure in CNT, is known from previous studies [16]. Due to their rounded structure, they can reduce the impact of pressure stresses on the bottom surface with the rolling effect [3]. CNTs play an important role in improving the tribological properties of materials due to their ease of rolling and unfolding. Also, their reduced size increases their capacity to fill in cracks and crevices [22, 24].

Furthermore, it was discovered that the favorable impact of Htc-G on the wear rate was extremely similar to that of Htc-G and CNT when carbon-based lubricant was added at a percentage of 0.2 wt%. This could be because it inhibits the tribofilm layer's ability to create nanoscale cracks and voids during the initial stages of wear. Since the morphology of graphite is not in a rounded form and is more prismatic, the decrease in the wear rate of the substrate material when graphite is used is lower than other carbons.

Profilometer images taken from the surface of the AlSi16 substrate after wear are given in Figure 5. When the profilometer images were examined in detail, it was observed that the first tests performed in pure boron oil had the deepest wear track in all wear tests. With the addition of carbon lubricants, it was observed that the pit depth decreased, but some indentation and protrusion occurred on the tracks. In particular, it is clearly seen on the surfaces of the specimens with Grpht and Htc-G. In the SEM analyses performed after the wear, it was seen that it was due to the adhesion of the fragments broken from the surface of the part to the surface, and this is explained below. These results show that carbon lubricants cause some abrasive wear. When HTC-C and CNT were used as solid lubricants, it was determined that the deterioration of the sample surface was minimal. This is thought to be due to the fact that it is the additive material with the smallest size morphology.

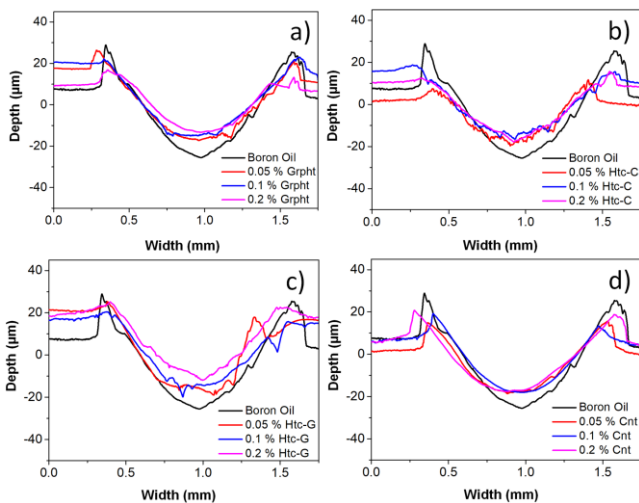


Figure 5. Two-dimensional profilometer images of substrate materials worn surfaces for a) Grpht, b) Htc-C, (c) Htc-G, and d) CNT

Figure 6 shows the SEM image obtained from the wear surface of the substrate sample with the use of boron oil. It is seen that small particles break off from the material surface and these debris cause the formation of abrasive wear mechanism. On the other hand, there is no obvious wear mark on the surface of the sample. SEM-EDX analysis shows that the reason for this is the oxide layer formed on the surface. In addition, it was determined that there are partially adhesive and oxidative parts.

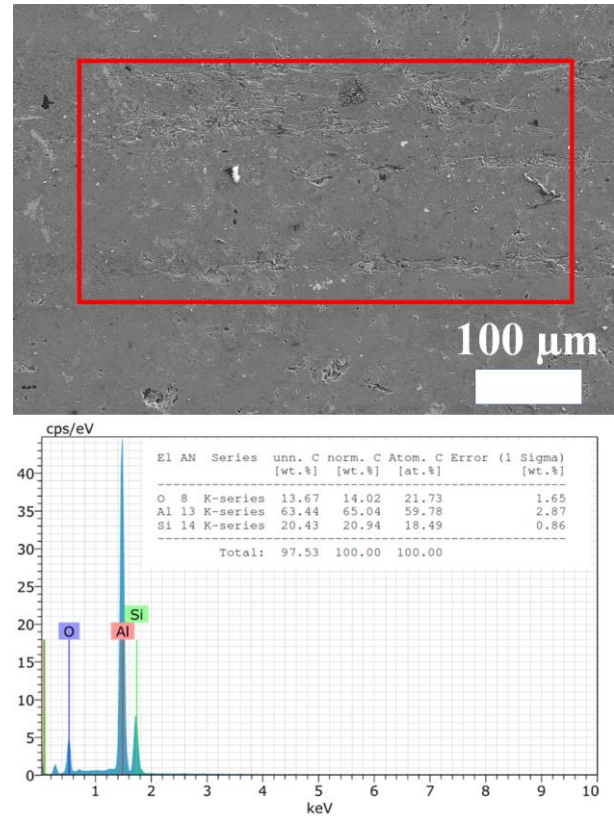


Figure 6. SEM image of AlSi16 Alloy surface after wear test in boron oil

Figure 7 shows the SEM image obtained from the substrate surface at the end of the wear test using Grpht solid lubricant. It is seen that oxidised residues (debris) are formed in regions 1,2 and 3 in the image. Oxygen peaks in EDX images also support this situation. In regions 4 and 5, it is seen that grooves are formed in the direction of sliding. Compared to the wear in boron oil environment, the deformation wear lines are more pronounced. The reason for this is that Grpht forms a lubricant film layer on the substrate material. This layer also reduces the force acting on the material surface. Due to the weak van der Waals bond between the carbon layers, the sliding of the layers on each other is facilitated, and this gives graphite self-lubricating properties and reduces wear [22].

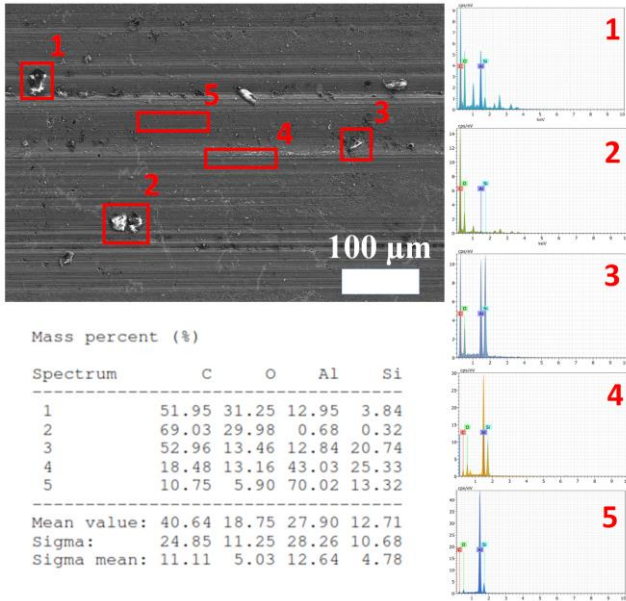


Figure 7. SEM image of AlSi16 Alloy surface after wear test in boron oil-Grpht

Figure 8 shows the SEM image obtained from the wear surface at the end of the test using Htc-C solid lubricant. In the SEM image, it is seen that oxidized carbon deposits are formed in regions 1, 2 and 3, and scratches parallel to the sliding direction are formed in regions 4 and 5. It was determined in the EDX analysis results that carbonaceous deposits and oxide structures were formed due to the heat generated during wear. Similar to the use of Grpht, it was observed that the abrasive and adhesive wear mechanisms were dominant on the substrate material.

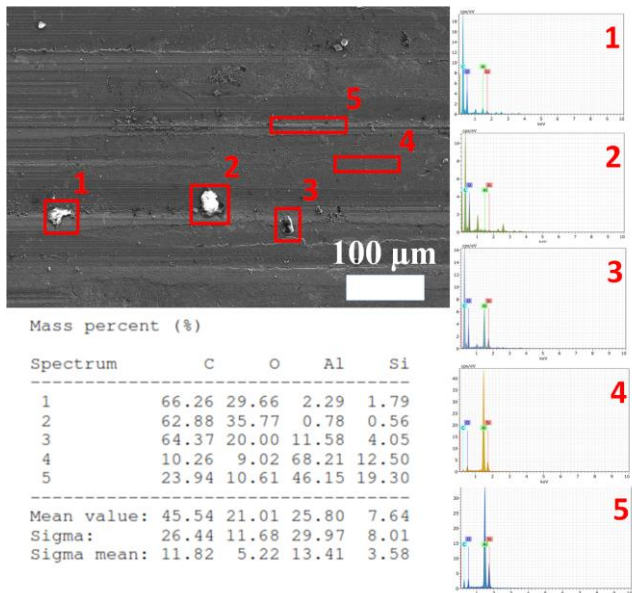


Figure 8. SEM image of AlSi16 Alloy surface after wear test in boron oil-Htc-C

Figure 9 shows the SEM image obtained from the substrate surface at the end of the wear test using Htc-G solid

lubricant. Similar findings were obtained when the previous carbons were used. According to SEM-EDX analyses, it was determined that carbonaceous deposits were formed on the surface. All surfaces analyzed contained at least 9.81 wt% carbon content.

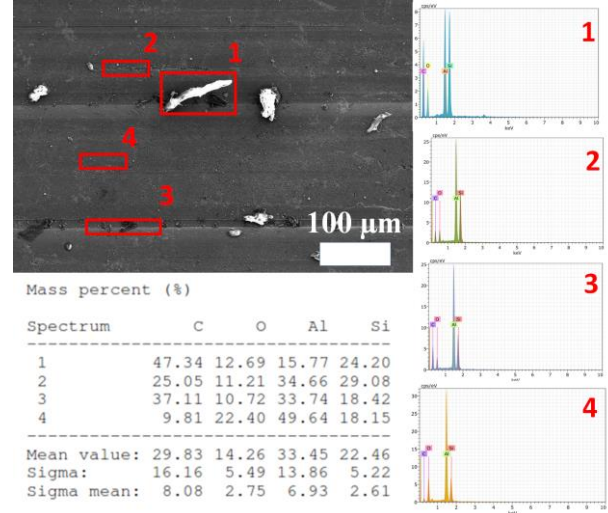


Figure 9. SEM image of AlSi16 Alloy surface after wear test in boron oil-Htc-G

Finally, Figure 10 shows the SEM image obtained from the wear surface at the end of the test using CNT solid lubricant. Similar to other carbon lubricants, oxidized carbon deposits (region 1) were observed. It is seen that the prominence of wear marks and the adhesive wear mechanism are reduced. The possible reason for this situation is explained in detail above. In the boundary lubrication regime, tribofilm formation, the squeeze-out, and the holding up of the lubrication film are very important. In particular, tribofilm formation was observed in all samples. Furthermore, no significant increase in temperature was observed throughout the wear tests. This supports the possibility that there may be no significant change in the viscosity of boron oil. Based on these findings, the lubrication regime where solid lubricant additives show their most pronounced effect can be classified as stable boundary lubrication [25, 26].

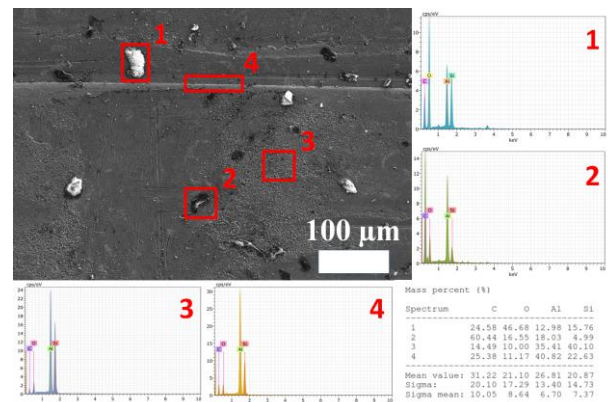


Figure 10. SEM image of AlSi16 Alloy surface after wear test in boron oil-CNT

4 Conclusion

In this study, carbon lubricants of four different morphologies were mixed with boron oil in three different ratios. It was found that the addition of carbon reduced the wear rate of the AlSi16 alloy at all ratios (approximately 20%-70%), and the addition at the highest ratio (0.2 wt%) reduced the wear rate the most. This was caused by the tribofilm formed on the substrate surface and the carbon filling the cavities at all ratios. When the performance of carbon lubricants was compared among themselves, it was determined that the best results were obtained with the use of CNT and Htc-C. Probably, since they have the smallest particles, they fill the cavities better than the other two carbons. For the same reason, it is thought that the rolling effect occurs with higher efficiency.

While CNT and HTC-C filled micro-grooves and reduced local strains because of their smaller particles, flaky graphite decreased wear by forming a lamellar coating film that covered surface defects. HTC-G, with the larger spherical morphology, functioned as rolling particles that minimized abrasive interaction. In summary, carbon additions with morphologies that might obscure surface irregularities or facilitate rolling motion exhibited the most efficient wear prevention properties.

Acknowledgement

The authors thank Karabuk University's BAP Office for financial support for the project Number: KBÜBAP-22-YL-069.

Conflict of interest

The authors declare they have no known competing financial interests or personal relationships.

Ethics declarations

During the preparation of this work, the authors used ChatGPT to improve the spelling, grammar, and style of the text. After using this tool/service, the authors reviewed and edited the content as needed and take full responsibility for the content of the publication.

Similarity ratio (iThenticate): %13

References

- [1] S. Wu, S. Tian, P. L. Menezes and G. Xiong, Carbon solid lubricants: role of different dimensions. *The International Journal of Advanced Manufacturing Technology*, 107:3875–95, 2020. <https://doi.org/10.1007/s00170-020-05297-8>.
- [2] N. Idusuyi and JI. Olayinka, Dry sliding wear characteristics of aluminium metal matrix composites: a brief overview. *Journal of Materials Research and Technology*, 8:3338–46, 2019. <https://doi.org/10.1016/j.jmrt.2019.04.017>.
- [3] Ö.E. Yurt, N. Sen, H. Simsir, Y. Kucuk, E. Altas, M.S. Gok, T. Civek, S. Korkmaz and M. H. Çetin, Investigation of tribological performance of hydrothermal carbon by pin-on-disc test and warm deep drawing process. *Surface Topography: Metrology and Properties*, 12:025019, 2024. <https://doi.org/10.1088/2051-672X/ad44b9>.
- [4] B. Bhushan, *Modern tribology handbook*, two volume set. CRC Press; 2000.
- [5] R.L. Deuis, C. Subramanian and J.M. Yellup, Dry sliding wear of aluminium composites—a review. *Composites Science and Technology*, 57:415–35, 1997. [https://doi.org/10.1016/S0266-3538\(96\)00167-4](https://doi.org/10.1016/S0266-3538(96)00167-4).
- [6] M.S. Zedalis, J.D. Bryant, P.S. Gilman and S.K. Das High-temperature discontinuously reinforced aluminum. *JOM*, 43:29–31, 1991. <https://doi.org/10.1007/BF03221100>.
- [7] A. Devaraju, A critical review on different types of wear of materials. *International Journal of Mechanical Engineering and Technology*, 6:77–83, 2015. https://iaeme.com/Home/article_id/IJMET_06_11_009.
- [8] S. Rzadkosz, J. Zych, M. Piękoś, J. Kozana, A. Garbacz-Klempka, J. Kolczyk and Ł. Jamrozowicz, Influence of refining treatments on the properties of Al-Si alloys. *Metalurgija*, 54:35–8, 2015. <https://hrca.k.srce.hr/126668>.
- [9] S. Khelge, V. Kumar, V. Shetty and J. Kumaraswamy, Effect of reinforcement particles on the mechanical and wear properties of aluminium alloy composites. *Materials Today: Proceedings*, 52:571–6, 2022. <https://doi.org/10.1016/j.matpr.2021.09.525>.
- [10] A. Erdemir and C. Donnet, Tribology of diamond-like carbon films: recent progress and future prospects. *Journal of Physics D: Applied Physics*, 39:R311, 2006. <https://doi.org/10.1088/0022-3727/39/18/R01>.
- [11] S. Mohan and A. Mohan, Wear, friction and prevention of tribo-surfaces by coatings/nanocoating. *Anti-Abrasive Nanocoatings*, 3-22, 2015. <https://doi.org/10.1016/B978-0-85709-211-3.00001-7>.
- [12] J. Sun and S. Du, Application of graphene derivatives and their nanocomposites in tribology and lubrication: a review. *RSC Advances* 9:40642–61, 2019. <https://doi.org/10.1039/C9RA05679C>.
- [13] D. Berman, A. Erdemir and A.V. Sumant, Few layer graphene to reduce wear and friction on sliding steel surfaces. *Carbon*, 54:454–9, 2013. <https://doi.org/10.1016/j.carbon.2012.11.061>.
- [14] B. Bourlon, D.C. Glatli, C. Miko, L. Forró and A. Bachtold, Carbon Nanotube Based Bearing for Rotational Motions. *Nano Letters*, 4:709–12, 2004. <https://doi.org/10.1021/nl035217g>.
- [15] X. Fan, Y. Xia, L. Wang and W. Li, Multilayer graphene as a lubricating additive in bentone grease. *Tribology Letters*, 55:455–64 2014. <https://doi.org/10.1007/s11249-014-0369-1>.
- [16] H. Simsir, N. Eltugral and S. Karagoz, Hydrothermal carbonization for the preparation of hydrochars from glucose, cellulose, chitin, chitosan and wood chips via low-temperature and their characterization. *Bioresource Technology*, 246:82–7, 2017. <https://doi.org/10.1016/j.biortech.2017.07.018>.

- [17] C. Falco, N. Baccile and M. M. Titirici, Morphological and structural differences between glucose, cellulose and lignocellulosic biomass derived hydrothermal carbons. *Green Chemistry*, 13:3273–81, 2011. <https://doi.org/10.1039/c1gc15742f>.
- [18] Ö. Karataş and T. Yüksel, Experimental investigation of the effects of boron oil additive in internal combustion engine. *Fuel*, 353:129234, 2023. <https://doi.org/10.1016/j.fuel.2023.129234>.
- [19] S. C. Tung and M.L. McMillan, Automotive tribology overview of current advances and challenges for the future. *Tribology International*, 37:517–36, 2004. <https://doi.org/10.1016/j.triboint.2004.01.013>.
- [20] A. A. Khan, M. S. Kaiser and M. Kaiser, Wear studies on Al-Si automotive alloy under dry, fresh and used engine oil sliding environment. *Research on Engineering Structures and Materials*, 9:1–18, 2023. <http://dx.doi.org/10.17515/resm2022.505ma0816>.
- [21] V. Ţucureanu, A. Matei and A.M. Avram, FTIR Spectroscopy for Carbon Family Study. *Critical Reviews in Analytical Chemistry*, 46:502–20, 2016. <https://doi.org/10.1080/10408347.2016.1157013>.
- [22] L. Zhang, J. Pu, L. Wang and Q. Xue, Frictional dependence of graphene and carbon nanotube in diamond-like carbon/ionic liquids hybrid films in vacuum. *Carbon*, 80:734–45, 2014. <https://doi.org/10.1016/j.carbon.2014.09.022>.
- [23] X. Liu, J. Pu, L. Wang and Q. Xue, Novel DLC/ionic liquid/graphene nanocomposite coatings towards high-vacuum related space applications. *Journal of Materials Chemistry A*, 1:3797–809, 2013. <https://doi.org/10.1039/C3TA00764B>.
- [24] V. Narayanunni, B. A. Kheireddin and M. Akbulut, Influence of surface topography on frictional properties of Cu surfaces under different lubrication conditions: Comparison of dry, base oil, and ZnS nanowire-based lubrication system. *Tribology International*, 44:1720–5, 2011. <https://doi.org/10.1016/j.triboint.2011.06.020>.
- [25] M. Kalin, I. Velkavrh and J. Vižintin, The Stribeck curve and lubrication design for non-fully wetted surfaces. *Wear*, 267:1232–40, 2009. <https://doi.org/10.1016/j.wear.2008.12.072>.
- [26] S. Stephan, S. Schmitt, H. Hasse and H.M. Urbassek, Molecular dynamics simulation of the Stribeck curve: Boundary lubrication, mixed lubrication, and hydrodynamic lubrication on the atomistic level. *Friction*, 11:2342–66, 2023. <https://doi.org/10.1007/s40544-023-0745-y>.

